


Self-running and self-floating two-dimensional actuator using near-field acoustic levitation

Cite as: Appl. Phys. Lett. **109**, 123503 (2016); <https://doi.org/10.1063/1.4963318>

Submitted: 17 August 2016 . Accepted: 12 September 2016 . Published Online: 21 September 2016

Keyu Chen, Shiming Gao, Yayue Pan, and Ping Guo 



View Online



Export Citation



CrossMark

ARTICLES YOU MAY BE INTERESTED IN

[Acoustic levitation of a large solid sphere](#)

Applied Physics Letters **109**, 044101 (2016); <https://doi.org/10.1063/1.4959862>

[The effect of acoustically levitated objects on the dynamics of ultrasonic actuators](#)

Journal of Applied Physics **121**, 114504 (2017); <https://doi.org/10.1063/1.4978365>

[Acoustic levitation of soap bubbles in air: Beyond the half-wavelength limit of sound](#)

Applied Physics Letters **110**, 121602 (2017); <https://doi.org/10.1063/1.4979087>



Measure Ready
M91 FastHall™ Controller

A revolutionary new instrument
for complete Hall analysis

 Lake Shore
CRYOTRONICS

Self-running and self-floating two-dimensional actuator using near-field acoustic levitation

Keyu Chen,¹ Shiming Gao,¹ Yayue Pan,² and Ping Guo^{1,a)}

¹Department of Mechanical and Automation Engineering, The Chinese University of Hong Kong, Hong Kong, China

²Department of Mechanical and Industrial Engineering, University of Illinois at Chicago, Chicago, Illinois 60607, USA

(Received 17 August 2016; accepted 12 September 2016; published online 21 September 2016)

Non-contact actuators are promising technologies in metrology, machine-tools, and hovercars, but have been suffering from low energy efficiency, complex design, and low controllability. Here we report a new design of a self-running and self-floating actuator capable of two-dimensional motion with an unlimited travel range. The proposed design exploits near-field acoustic levitation for heavy object lifting, and coupled resonant vibration for generation of acoustic streaming for non-contact motion in designated directions. The device utilizes resonant vibration of the structure for high energy efficiency, and adopts a single piezo element to achieve both levitation and non-contact motion for a compact and simple design. Experiments demonstrate that the proposed actuator can reach a 1.65 cm/s or faster moving speed and is capable of transporting a total weight of 80 g under 1.2 W power consumption. *Published by AIP Publishing.* [<http://dx.doi.org/10.1063/1.4963318>]

Non-contact actuators are widely employed in precision machine-tools, nanotechnology, and metrology for their low friction, high precision, low wear, and low noise. Air bearings and electromagnetic bearings, for instance, have been extensively studied and applied as a kind of non-contact actuator.^{1,2} However, these non-contact actuators have their drawbacks, such as complex design, high costs, constrained moving ranges, electromagnetic interference, undesirable noise, requirement of clean air, etc.

In near-field acoustic levitation, heavy objects can be levitated in a near-field region (several to several hundred microns) by an acoustic radiation force, whose amplitude is inversely proportional to the square of levitation height.³ Specifically, a surface vibrating at an ultrasonic frequency is usually used to provide the acoustic levitation force.⁴ Furthermore, when the acoustic streaming is produced within the air gap between the substrate and the levitated object, the object can be driven by a viscous force of air to achieve non-contact transportation.^{3,5,6} However, due to the use of rails, these devices are limited by their complicated design, large power consumption, and constrained moving direction and range. Alternatively, the levitated object can be excited to generate acoustic pressure to act as a self-floating or self-running stage. The non-contact self-transportation is achieved by creating a traveling wave on the oscillating object or by asymmetric vibration of the object in order to introduce acoustic streaming.⁷⁻⁹ Though the self-running stage can overcome the restrictions of guide rails, many problems that prevent this technology from being adopted still exist. These self-running stage designs mainly suffer from low energy efficiency, complicated and redundant vibration sources, and difficulties in trajectory control.⁷⁻⁹

Facing these technical drawbacks, we propose a novel self-floating and self-running two-dimensional actuator utilizing the principles of near-field acoustic levitation and coupled resonant vibration. The actuator adopts a compact design using a single piezoelectric element to achieve the triple functions of levitation and motion in two dimensions to achieve high efficiency, high controllability, and unlimited traveling range. If combined with further development of real-time feedback and control systems, the proposed design has great potential in the areas of linear bearings, high-precision machine tools, metrology, mobile robots, next-generation hovercars, etc.

The proposed actuator design could float against a flat ground using near-field acoustic levitation; meanwhile, it could generate acoustic streaming at a controlled direction within the thin air gap between the actuator and ground to achieve non-contact motion, as illustrated in Fig. 1(a). The coupled resonant vibration of the structure is utilized to achieve self-floating and self-running with high energy efficiency. The structure has a longitudinal vibration mode, as well as a bending mode as illustrated in Fig. 1(b). The structure is carefully designed so that the resonant frequencies of the two modes, namely, the first longitudinal and the second bending modes, are identical. Coupled resonant vibration, or superposition of the two normal modes, can be achieved by exciting the structure at the coupled resonant frequency with proper excitation signals, as shown in Fig. 1(b). Ideally, if two halves of the piezoelectric ring are excited with sinusoidal signals with a phase difference at 90°, both modes will be equally excited to generate an elliptical vibration. Elliptical vibration using coupled resonant modes has been widely adopted in other areas, such as ultrasonic motors¹⁰⁻¹² and elliptical vibration cutting.^{13,14}

The asymmetric vibration due to the elliptical vibration creates acoustic streaming, enabling non-contact transportation

^{a)} Author to whom correspondence should be addressed. Electronic mail: pguo@mae.cuhk.edu.hk

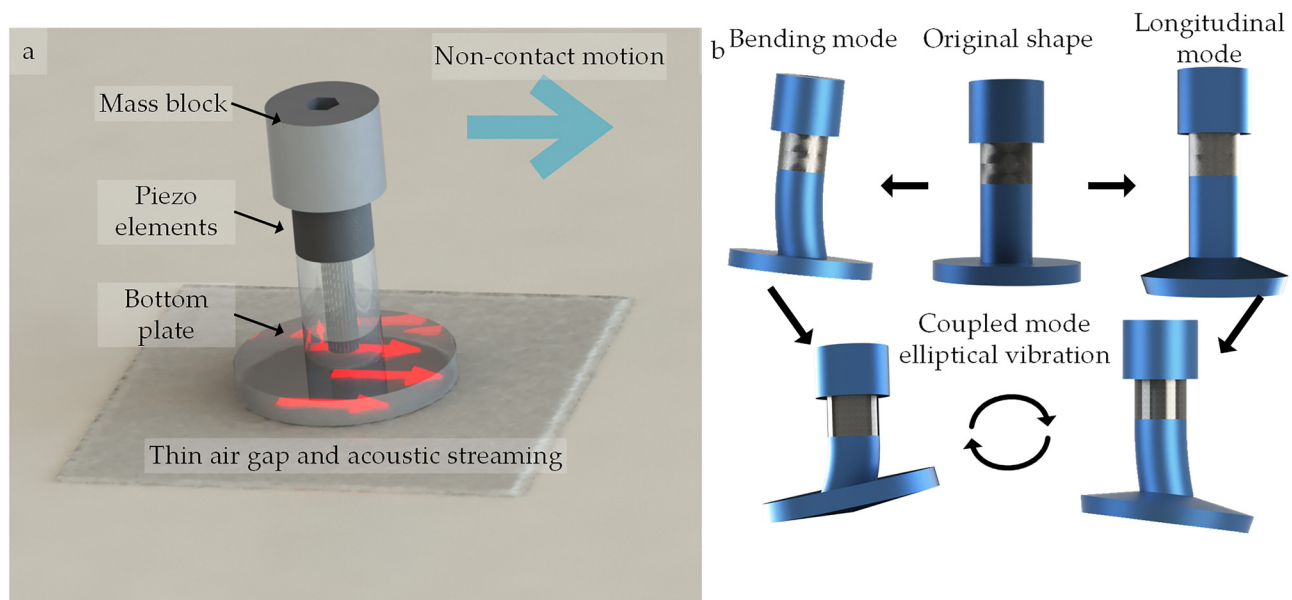


FIG. 1. Operation principle of the self-floating and self-running actuator: (a) component description and schematic of non-contact transportation and (b) schematic of coupled resonant vibration.

of the floating object. It can be intuitively explained by the exhaust and suction strokes during each cycle of vibration. During the compression stage of the vibration cycle as shown in Fig. 2(a), the actuator elongates and moves downwards in a diagonal direction to compress the air. Due to the slope angle of the bottom plate, the net reaction force from the air produces a lateral force to push the actuator towards the right. During the expansion stage of the cycle shown in Fig. 2(b), the actuator contracts and moves upwards in the other diagonal direction. Similarly, since the bottom plate leans towards the left, the forced air expansion produces a net lateral force also towards the right. For both the compression and expansion stages, the reaction force applied on the bottom plate has a lateral component pointing to the right, resulting in non-contact motion.

By flipping the excitation sequence of the longitudinal and bending modes, thus to change the elliptical vibration direction, one-dimensional reverse motion of the actuator can be achieved. Furthermore, since the actuator structure is axially symmetric, two-dimensional motion of the actuator can be implemented by adjusting the combination of excitation signals on the different segments of piezoelectric rings

to activate the bending mode of the structure in the orthogonal direction.

Modal analysis results in ANSYS were used to guide the optimal design of the structure. Dimensions of the top mass block (diameter and length), as well as the bottom plate (diameter and length), were varied to tune the resonant frequencies of the two relevant modes. The goal was to match the resonant frequencies of the first longitudinal and second bending modes. The coupled resonant frequency was further constrained to avoid disturbing noises during the operation at an ultrasonic frequency. After several iterations of optimization, the longitudinal mode was identified at 20.73 kHz. The simulated mode shape is shown in Fig. 3(a). Additionally, the second bending mode was identified at 21.33 kHz, and its corresponding mode shape simulation is shown in Fig. 3(b). Due to the symmetry of the structure, there is an identical bending mode in the orthogonal direction at the same frequency (21.33 kHz).

To further study the principle of non-contact self-transportation, acoustic pressure distribution in the thin layer of air between the moving actuator and the ground was studied

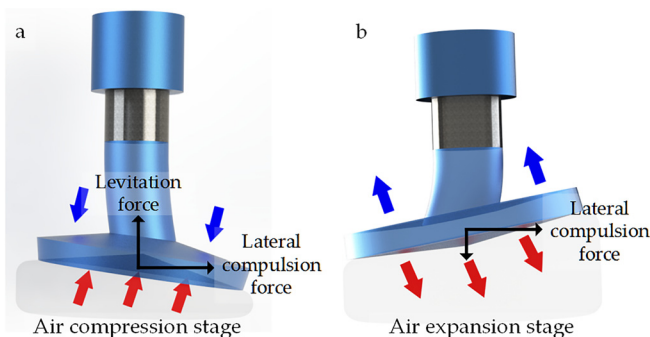


FIG. 2. Principles of non-contact motion due to the (a) air compression stage and (b) air expansion stage.

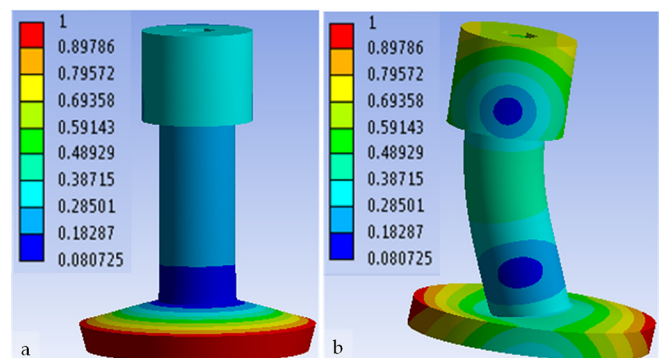


FIG. 3. Resonant mode shapes of the stage predicted by finite element analysis: (a) longitudinal mode @ 20.73 kHz and (b) bending mode @ 21.33 kHz (the color bar indicates the normalized deformation of the structure.)

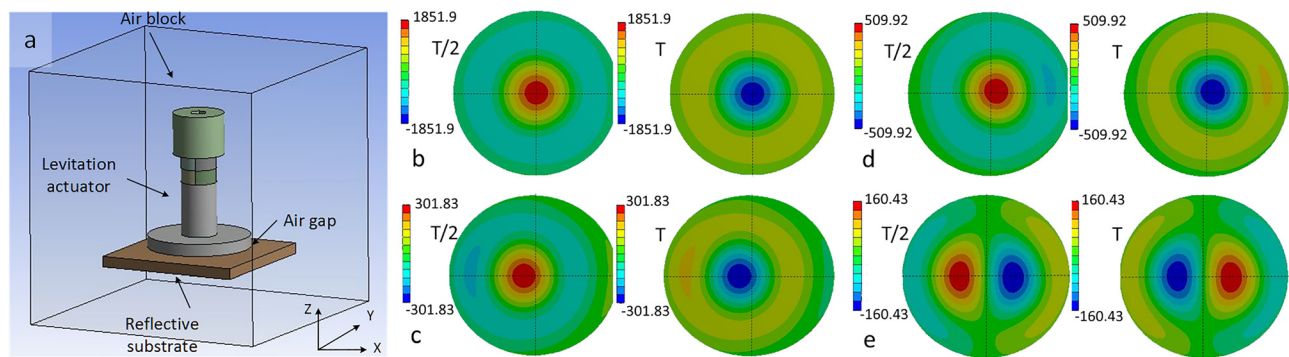


FIG. 4. Piezoelectric-structural-acoustic simulation: (a) model description and representative acoustic pressure distributions within a period for the phase angle of (b) 0° , (c) 45° , (d) 90° , and (e) 180° .

via piezoelectric-structural-acoustic-coupled simulation in ANSYS, as shown in Fig. 4(a). The two excitation inputs were set the same as those in the harmonic analysis, where the voltage amplitude was 200 V and the frequency was 21 kHz. The phase angle between the two inputs was set at 0° , 45° , 90° , and 180° , which correspond to the results shown in Figs. 4(b)–4(e). For the pure longitudinal mode shown in Fig. 4(b), the spot with the largest variation of air pressure coincides with the geometric center of the bottom plate, which results in stable levitation of the actuator. For the pure bending mode shown in Fig. 4(e), though air pressure distribution is non-uniform at any specific time, its average value over a cycle is symmetric about the center axis, which contributes to the stable levitation. For coupled vibration of the longitudinal and bending modes, the maximal pressure point deviates from the geometric center and moves along the center axis during each cycle, which creates a pseudo-traveling wave (supplementary material Movie S1).

We made a prototype of a self-floating and self-running actuator based on the design shown in Fig. 1. The critical dimensions of the structure were obtained from the simulation results, as discussed in the above paragraphs. The excitation condition for the self-running mode was identified at

21.07 kHz with a 40° phase angle difference between the two excitation signals. It was observed that the optimal working condition was quite wide in range, as shown in Figs. 5(a) and 5(c), where a phase angle between 25° and 40° gave similar performance.

To study the influence of the input parameters on the actuator performance, two sets of experiments were conducted to record the velocity and thrust force of the actuator (see supplementary material for details of the experimental setup and procedures). The excitation frequency was kept at the optimal value, while the input voltage and the phase angle between the two excitation signals were varied. For both the velocity and the thrust force tests, the voltage amplitude was varied from 120 V to 220 V, and the phase angle difference was varied from 10° to 55° . The results are summarized and plotted in Fig. 5. As shown in Fig. 5(a), the velocity response to the phase angle is symmetric about the Y-axis, which indicates that by simply flipping the input phase angle, bi-directional motion with identical performance can be achieved (supplementary material Movies S2 and S3). The moving velocity reaches its maximum at 1.65 cm/s with a 25° phase angle, then stabilizes, and gradually decreases with the further increase in the input phase angle. When the input phase angle was fixed

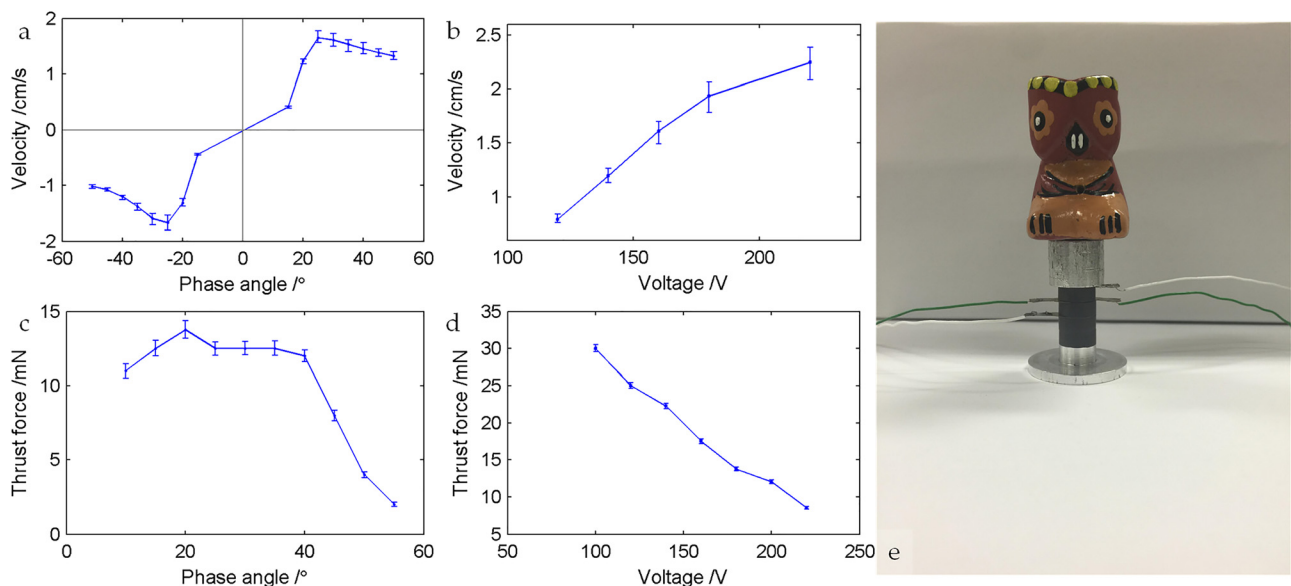


FIG. 5. Performance of the proposed self-running actuator: influence of (a) input phase angle and (b) voltage amplitude on the actuator velocity; influence of (c) input phase angle and (d) voltage amplitude on the actuator thrust force; (e) actuator with a load.

at 40° and the voltage amplitude was adjusted, the actuator velocity increased with the voltage and reached 2.25 cm/s at 220 V in our experiments. By comparing the influence of input phase angle on the actuator velocity and thrust force (Figs. 5(a) and 5(c)), we found a similar plateau on the curve, where the optimal range of input phase angle is determined between 25° and 40°. Fig. 5(d) indicates that the maximal thrust force is inversely proportional to the input voltage, which determines the levitation height, since acoustic streaming will be decreased for an enlarged air gap.⁹ It should be noted that the actuator performance not only depends on the excitation signals, but also on the surface roughness and textures of the bottom plate and the ground. Rough surfaces and stains would reduce the actuator velocity and levitation height.

In summary, we have presented a novel design, which utilizes only a single actuator to achieve the levitation and controlled two-dimensional motion with identical performance. Furthermore, the proposed device is highly energy efficient such that it can achieve non-contact transportation of its own weight of 20.13 g under 1.2 W at 1.65 cm/s or even faster. The maximal thrust force of 30 mN was achieved with the proposed design. We have also loaded the actuator with additional masses such that the actuator can still be levitated and moved at a total weight of 80 g (Fig. 5(e)). This energy-efficient and unique design of the device (elimination of guide rails) opens up numerous exciting applications, including the following: (1) the actuator can be easily adapted to be a two-dimensional positioning stage if an encoder and feedback control system are installed; (2) the actuator could have batteries, driving circuits, and sensors integrated in the device to become an autonomous mobile robot; and (3) the actuator can be scaled-up to become the next-generation hovercar. To realize any meaningful application for the proposed actuator

design, many technical challenges still remain to be tackled in our future work, including modeling of the system dynamics, development of a two-dimensional surface encoder and feedback control system, and characterization of closed-loop positioning accuracy and repeatability of the actuator.

See [supplementary material](#) for details of the experimental setup and procedures.

This work has been supported by the Innovation and Technology Fund, Hong Kong, Grant No. ITS/014/15, and the start-up fund provided by the Faculty of Engineering, The Chinese University of Hong Kong.

¹W.-J. Kim and D. L. Trumper, *Precis. Eng.* **22**(2), 66 (1998).

²K. S. J. Pister, R. S. Fearing, and R. T. Howe, paper presented at the Micro Electro Mechanical Systems: Proceedings, An Investigation of Micro Structures, Sensors, Actuators, Machines and Robots (IEEE, 1990).

³Y. Hashimoto, Y. Koike, and S. Ueha, *J. Acoust. Soc. Am.* **103**(6), 3230 (1998).

⁴E. Matsuo, Y. Koike, K. Nakamura, S. Ueha, and Y. Hashimoto, *Ultrasonics* **38**(1), 60 (2000).

⁵X. Li, Y. Sun, C. Chen, and C. Zhao, *IEEE Trans. Ultrason. Ferroelectr. Freq. Control* **57**(4), 951 (2010).

⁶S. Ueha, Y. Hashimoto, and Y. Koike, *Ultrasonics* **38**(1), 26 (2000).

⁷D. Koyama, K. Nakamura, and S. Ueha, *IEEE Trans. Ultrason. Ferroelectr. Freq. Control* **54**(11), 2337 (2007).

⁸D. Koyama, H. Takei, K. Nakamura, and S. Ueha, *IEEE Trans. Ultrason. Ferroelectr. Freq. Control* **55**(8), 1823 (2008).

⁹D. Koyama and K. Nakamura, *Jpn. J. Appl. Phys.* **48**(7S), 07GM07 (2009).

¹⁰J. Wallaschek, *Smart Mater. Struct.* **7**(3), 369 (1998).

¹¹K. Uchino, *Smart Mater. Struct.* **7**(3), 273 (1998).

¹²H. Storck, W. Littmann, J. Wallaschek, and M. Mracek, *Ultrasonics* **40**(1), 379 (2002).

¹³E. Shamoto and T. Moriwaki, *CIRP Ann. Manuf. Technol.* **48**(1), 441 (1999).

¹⁴P. Guo and K. F. Ehmann, *Precis. Eng.* **37**(2), 364 (2013).